Electrical Stimulation of Myoblast Proliferation and Differentiation on Aligned Nanostructured Conductive Polymer Platforms (1)

DATASET · JANUARY 2013

READS
29

11 AUTHORS, INCLUDING:

Anita Quigley
University of Wollongong and University of …
45 PUBLICATIONS **497** CITATIONS
SEE PROFILE

Joselito M Razal
University of Wollongong
79 PUBLICATIONS **2,616** CITATIONS
SEE PROFILE

Magdalena Kita
University of Wollongong
22 PUBLICATIONS **294** CITATIONS
SEE PROFILE

Robert Kapsa
University of Wollongong-St Vincent's Hosp…
73 PUBLICATIONS **1,434** CITATIONS
SEE PROFILE

Electrical Stimulation of Myoblast Proliferation and Differentiation on Aligned Nanostructured Conductive Polymer Platforms

Anita F. Quigley, Joselito M. Razal, Magdalena Kita, Rohoullah Jalili, Amy Gelmi, Anthony Penington, Raquel Ovalle-Robles, Ray H. Baughman, Graeme M. Clark, Gordon G. Wallace, and Robert M. I. Kapsa**

Appropriate control of cellular growth is critical for tissue engineering applications and for the design of effective bioelectronic interfaces for bionic applications. Recent studies have shown that platforms with micro-[1,2] and nanostructured[3,4] surfaces provide topographical cues that can positively influence cellular response in vitro. For example, the use of aligned electrospun nanofibers has resulted in orientated cellular differentiation of bone marrow stromal cells with increased levels of mineralization[5] and differentiation of mesenchymal stem cells towards a neural lineage.[6] Similarly, for skeletal muscle engineering and nerve regeneration applications, nanofibrous and microstructured surfaces have afforded directionality suitable to both muscle fiber orientation[7,8] and axonal growth.[9] More recently, platforms that incorporate micro and nanostructured conducting polymers (CPs) and carbon nanotubes (CNTs) for the guidance and stimulation of several cell types have been reported.[10–14] CPs are of particular interest because they provide the means to deliver biological agents while enabling simultaneous delivery of relevant electrical stimulation for modulating cell/tissue development.[15,16] In particular, polypyrrole (PPy) has been utilized in a number of in vitro studies investigating nerve,[17] muscle,[18] bone,[19] and endothelial cell growth.[20] Collectively, these studies reveal that the level of cytocompatibility and cell-material interaction may be modulated by the following external influences: (1) physical stimulation via controlled surface roughness, channels, or grooves; (2) biochemical stimulation via the release of biological growth factors; (3) mechanical stimulation and (4) electrical stimulation. Likewise, CNTs have been considered ideal candidate materials for bionics applications because of their inherent electrical conductivity and mechanical properties. When suitably functionalized, CNTs have shown improved compatibility with a variety of cell types including mesenchymal stem cells[21] and neural cells.[22] Multiwalled carbon nanotubes (MWNT) can be fashioned into nanostructured conducting templates, such as "aerogel sheets" as originally described by Zhang.[23] This process involves drawing bundles of nanotubes from the side wall of the MWNT forest so that they join with bundled nanotubes that have reached the top and bottom of the forest, resulting in long fibrils with minimal breaks. These linearly arranged fibrils form aerogel sheets that are highly conductive and exhibit linear nanostructure. Linear arrays of laminin-coated aligned MWNT sheets (aerogel sheets) have also been shown effective in guiding axonal outgrowth from dorsal root ganglia[24] and more recently, in directing the growth alignment of Chinese hamster ovary cells.[14]

Similarly to nerve, a major consideration for the engineering of muscle is the ability to restore tissue in an appropriate orientation reflecting the native state. In particular, myotubes must be engineered in a linear array to reflect native muscle structure, which is organized as highly linear, unbranched bundles in vivo. This organization is in part mediated through the physical and biological properties of the extracellular matrix (ECM). The ECM of skeletal muscle consists of a nanofibrous network of proteins.[25] This linearized structure has been replicated ex vivo resulting in the linear orientation of differentiated primary skeletal muscle cells grown on microstructured CP platforms.[18] This effect has also been achieved at the nanoscale using biodegradable nanofibers,[8] demonstrating that nanoengineered scaffolds provide the ability to control muscle fiber orientation. The use of CPs in an orientated, nanostructured scaffold for muscle engineering could constitute the ideal substrata as it is documented that electrical stimulation of muscle cells on CP substrates can elicit molecular and behavioural changes to myoblasts favouring differentiation.[26–28] Therefore the current study utilizes CP templates to investigate how the effects of aligned nanotopography in conjunction with charge-balanced biphasic

Dr. A. F. Quigley,[+] Dr. J. M. Razal,[+] M. Kita, R. Jalili, A. Gelmi, Prof. G. M. Clark, Prof. G. G. Wallace, Prof. R. M. I. Kapsa
ARC Centre of Excellence for Electromaterials Science
Intelligent Polymer Research Institute
Innovation Campus, Squires Way
North Wollongong NSW 2522, Australia
E-mail: gwallace@uow.edu.au; rmik@unimelb.edu.au

Dr. A. F. Quigley, M. Kita, Prof. A. Penington, Prof. R. M. I. Kapsa
Centre for Clinical Neuroscience and Neurology
Research and Department of Medicine
The University of Melbourne
St. Vincent's Hospital, 41 Victoria Pde
Fitzroy, VIC 3065, Australia

Dr. R. Ovalle-Robles, Prof. R. H. Baughman
Alan G. MacDiarmid NanoTech Institute
University of Texas at Dallas
Richardson, Texas 75080, USA

[+] Dr. A. F. Quigley and Dr. J. M. Razal contributed equally to this work.

DOI: 10.1002/adhm.201200102

ADVANCED HEALTHCARE MATERIALS
www.advhealthmat.de

Materials Views
www.MaterialsViews.com

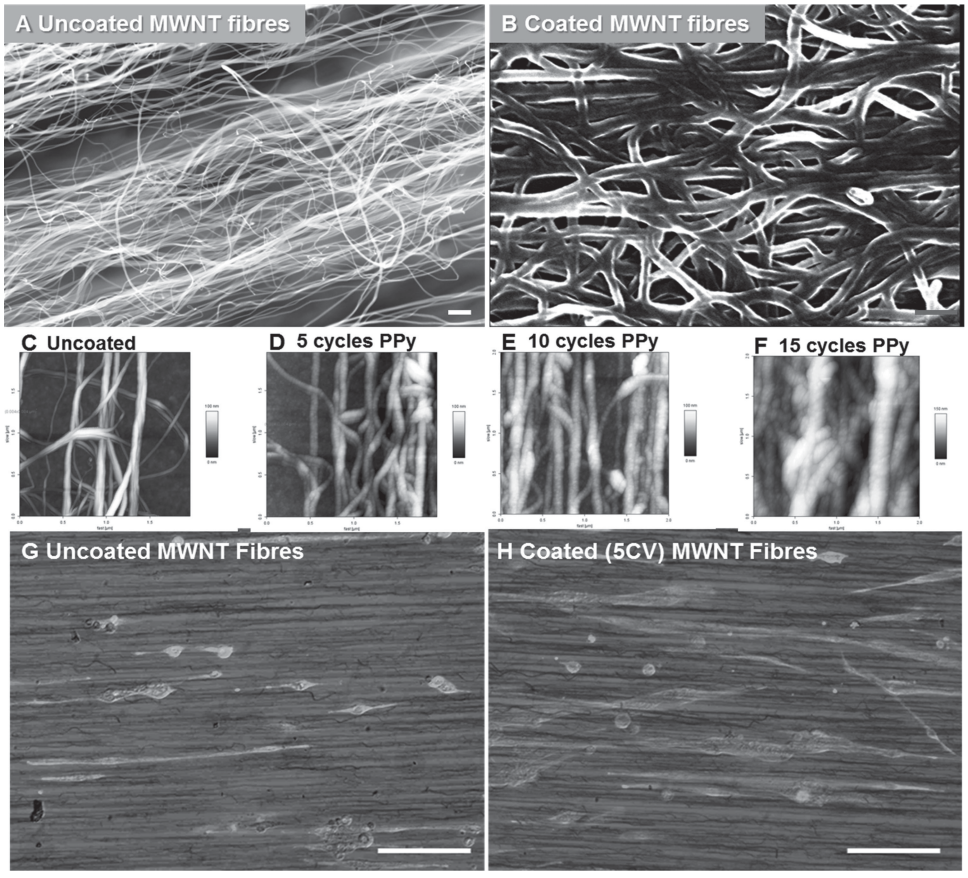

Figure 1. AFM and SEM images of MWNT and MWNT/PPy-*p*TS nanostructured scaffolds. MWNT were arrayed in a linear manner on Au mylar surfaces (A) to facilitate myotube orientation. PPy-*p*TS coating of MWNT fibers shows an even distribution of PPy-*p*TS (B). Increasing cycles of PPy-*p*TS deposition results in increased fiber thickness as demonstrated by AFM (C–F). The linear directionality of the uncoated (G) and coated MWNT fibers (H) can be seen by differential interference contrast light microscopy (myotubes are fluorescently labelled for desmin in panels G and H, scale bars represent 100 µm).

constant current stimulation (as used in nerve cultures[11,12]) influences the orientation and growth behaviour of primary myoblasts in vitro.

Novel nanostructured conducting scaffolds consisting of aligned MWNT with and without *para*-toluene sulphonic acid doped PPy (PPy-*p*TS) coatings were synthesized for this purpose (**Figure 1**). *p*TS is an organic compound that acts as a dopant facilitating the polymerization of PPy from pyrrole monomers.[29] *p*TS was selected as a dopant in the current study on the basis of our observations that PPy-*p*TS films have excellent mechanical properties and provide a suitable substrate for the growth of primary muscle cells.[29,30] Analysis of the electrochemical behaviour of these platforms revealed an enhancement in the electrochemical activity of the MWNTs upon deposition of PPy-*p*TS, attributed to the expected oxidation-reduction of the polymer occurring during the potential sweep (**Figure 2**). Similarly enhanced electrochemical profiles were obtained for PPy-*p*TS coated gold mylar (Au mylar) substrates.

To determine the behaviour of muscle cells on these surfaces, primary murine myoblasts were seeded onto the

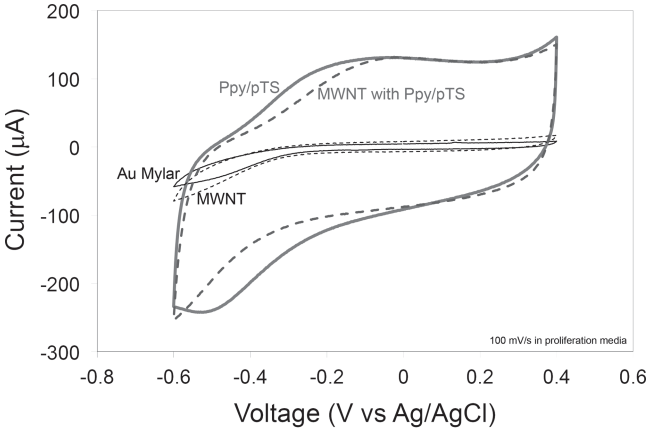

Figure 2. CV analysis of scaffolds revealed significant differences between MWNT substrates without PPy-*p*TS coatings and PPy-*p*TS coated substrates. MWNT deposited on Au mylar (thin dotted line) showed a similar CV profile to Au mylar (thin unbroken line) whilst PPy-*p*TS coated MWNT (thick dotted line) showed a significant increase in redox potential, similar to that of PPy-*p*TS surfaces with no underlying MWNT layer (thick unbroken line).

DOI: 10.1002/adhm.201200102

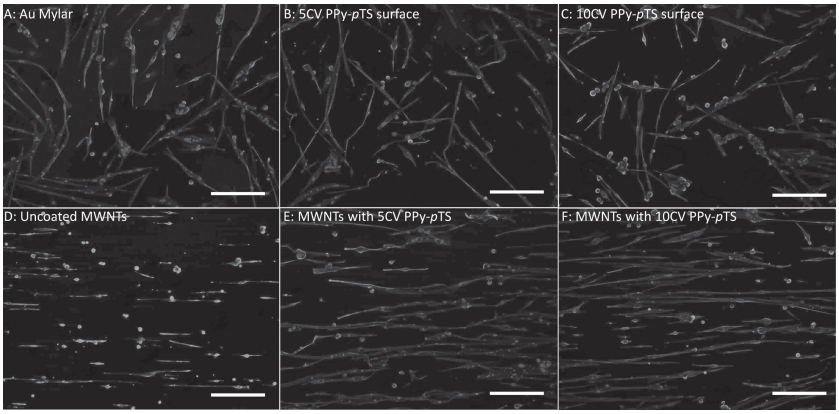

Figure 3. Primary muscle myoblasts differentiated on MWNT and MWNT/PPy-*p*TS scaffolds. Myoblasts differentiated on conductive surfaces were fluorescently labelled for desmin. Myotubes demonstrated a random orientation on Au mylar (A) and PPy-*p*TS surfaces (5 and 10 CV cycles, B and C) without underlying nanostructure. In contrast, myotubes differentiated on MWNT (D), and PPy-*p*TS coated MWNT (E and F) surfaces demonstrated alignment with the MWNT array. Scale bars = 100 µm.

scaffolds. Myoblasts attached, proliferated and differentiated on all prepared surfaces without the use of adhesion molecules (**Figure 3**). After 6 days under differentiation conditions, myotube alignment, length, surface area, differentiation and total cell number (total nuclei/mm^2) was assessed. Myotubes grown on PPy-*p*TS and Au mylar exhibited a random orientation, as expected (Figure 3a–c), however myotubes grown on nanostructured surfaces exhibited alignment (Figure 3d–f). An increase in myotube alignment ($p < 0.001$) was observed on uncoated MWNT platforms compared to smooth surfaces of Au mylar and PPy-*p*TS with 91.3% of myotubes demonstrating alignment varying between 0 to 5 degrees relative to MWNT orientation (**Figure 4**a). A significant increase in myotube alignment was also observed on linear MWNT/PPy-*p*TS arrays compared to Au mylar and PPy-*p*TS ($p < 0.001$). The extent of myotube alignment was found to decrease with increasing PPy-*p*TS thickness with a significant reduction in alignment seen on MWNT surfaces coated with 5 ($p < 0.05$), 10 ($p < 0.05$) and 35 cyclic voltammetry (CV) cycles of PPy-*p*TS deposition ($p < 0.001$).

Myotube length, size and differentiation status was determined by morphometric analysis. An average myotube length of around 321–353 µm was measured on smooth (Au mylar and PPy-*p*TS) and PPy coated nanostructured platforms (MWNT/PPy-*p*TS), with no significant differences in length found between platforms (Figure 4b). However, myotubes grown on uncoated MWNT arrays were significantly shorter than myotubes grown on non-nanostructured surfaces and MWNT/PPy-*p*TS arrays, with an average myotube length of 257 µm. The deposition of PPy-*p*TS seemed to alleviate this effect with a significant increase in myotube length between MWNT and MWNT/PPy-pTS at both 5 and 10 CV cycles ($p < 0.05$). These results were also reflected in measurements of "myotube footprint" area (myotube size) where myotubes had a significantly lower footprint on uncoated MWNT arrays (Figure 4c). Again, the deposition of PPy-*p*TS over the MWNT array resulted in a significant increase in myotube footprint area ($p < 0.05$), similar to levels observed on smooth (Au mylar and PPy-*p*TS) platforms. The higher myotube length and surface area observed on MWNT/PPy-*p*TS, suggests that the deposition of PPy-*p*TS improved the cytocompatibility of the platforms, which should be reflected in the level of myoblast fusion or differentiation. A significantly lower multinucleation density was observed on MWNT arrays without PPy-*p*TS coatings compared to all other platforms analysed ($p < 0.001$, Figure 4d). A lower cell density was also observed on the uncoated MWNT platforms, however this did not reach statistically significant levels (Figure 4e). This indicates that the level of myotube differentiation can be improved through PPy-*p*TS deposition. These results suggest that the presence of PPy-*p*TS coatings on MWNT templates increases compatibility with myotubes and/or myoblasts, therefore, nanostructured arrays with minimal (5 CV cycles) PPy-*p*TS coatings were chosen as the preferred platforms for subsequent electrical stimulation studies, due to the minimal disruption of nanostructure.

For electrical stimulation experiments, primary murine myoblasts were seeded onto MWNT platforms coated with 5 CV cycles of PPy-*p*TS and electrically stimulated in differentiation media. A significant increase in cell density was seen in the electrically stimulated group ($p < 0.001$, **Figure 5**a) from 699.6 ± 55.69 to 965.5 ± 49.04 cells/mm^2, corresponding to an increase of 38%. In addition, a significantly higher level of myotube formation occurred in the electrically stimulated group (67.9% of nuclei in multinucleate structures) compared to non-stimulated controls (60.4% multinucleation; $p < 0.001$, Figure 5b), representing an empirical difference of 7.5% of total nuclei participating in myofiber multinucleation, or approximately 12.4% greater myodifferentiation with electrical stimulation than without. This simultaneous increase in cell density and myotube formation suggests augmentation in proliferation and differentiation by electrical stimulation. In addition, an analysis of average desmin positive surface area (SA) per nuclei (representing both myoblasts and myotubes) revealed no difference between stimulated and non-stimulated samples, suggesting that in the current study electrical stimulation does not affect cell spreading (Supporting Information, Figure S1).

Various polymers, both biologically derived and synthetic, have been used to create micro and nanostructured templates to influence cell behaviour. CPs are of particular relevance to tissue engineering and bionic applications as they show excellent biocompatibility,[31] can be chemically functionalized,[32] store and release trophic factors,[17] deliver electrical stimulus[11] and can be modified to sense biological events.[33] Our laboratories have been investigating the use of micro and nanostructured CPs for tissue interfacing and bionic applications, particularly for influencing the growth and differentiation of neural and muscular tissues.[11,16,18,20,30,34,35] These polymers have application in the development of bionic devices, which may require cell seeding ex vivo prior to implantation to facilitate tissue integration and interfacing. Alternatively, bionic devices may need to encourage cell migration or axonal growth into a device and, as such, be specifically designed to encourage infiltration by

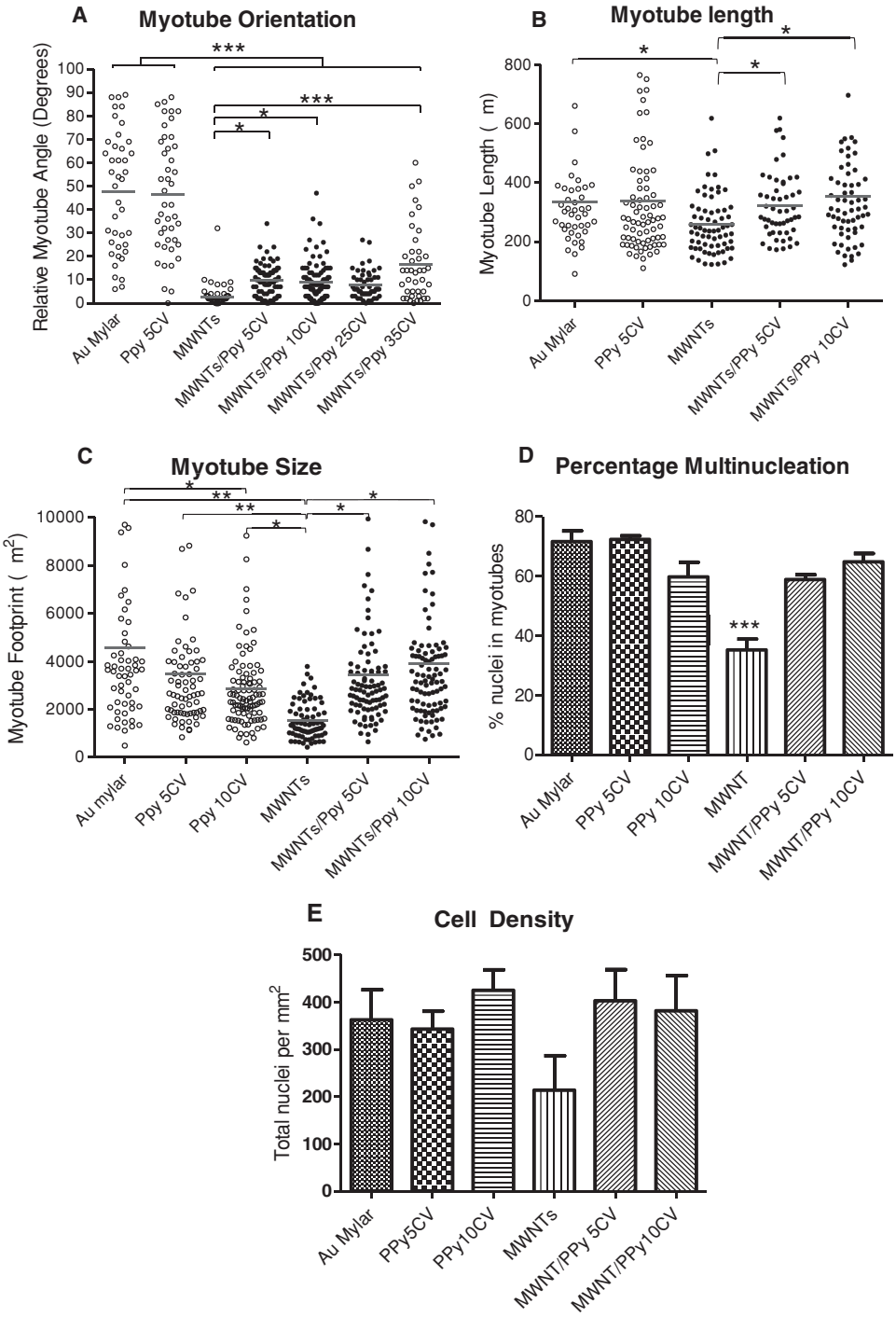

Figure 4. Analysis of myotube orientation and characteristics on nanostructured scaffolds. Myotubes differentiated on Au mylar and PPy-*p*TS demonstrated a random orientation, however a significant increase in myotube orientation was seen on MWNT surfaces, as well as PPy-*p*TS with an underlying layer of MWNT (A). Increased deposition of PPy-*p*TS on MWNT surfaces significantly reduced the degree of alignment observed on MWNT platforms, suggesting some loss of orientated nanostructure. Myotube length was significantly reduced on MWNT surfaces; however this effect was significantly ameliorated by the deposition of PPy-*p*TS (B). Similarly, myotube size (myotube footprint) was significantly reduced on MWNT surfaces, deposition of PPy-*p*TS (5 and 10 CV cycles) on MWNT resulted in significant increases in myotube size (C). The percentage of nuclei in myotubes (i.e., myoblast differentiation) was also significantly reduced on MWNT surfaces compared to Au mylar and PPy-*p*TS (D). Cell density was lower on MWNT surfaces, however this did not reach a statistically significant level (E). This effect was ameliorated through coating of MWNT surfaces with 5 and 10 CV cycles of PPy-*p*TS. Error bars represent standard error of the mean (SEM).

the host tissues. These properties can be achieved by inclusion of biological elements such as cell adhesion molecules or trophic factors and, at a more fundamental level, by the use of topographic directional cues. We have previously demonstrated that conductive polymers can influence neural behaviour through microstructure, electrical stimulation and release of

DOI: 10.1002/adhm.201200102

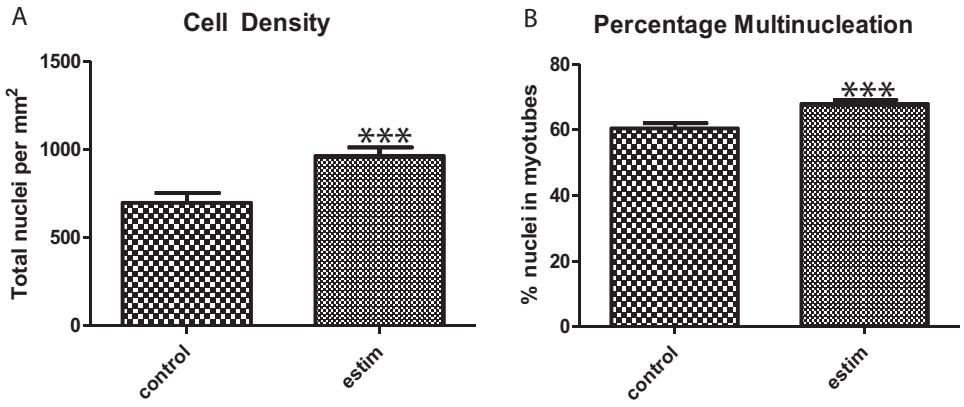

Figure 5. Electrical stimulation of myoblasts on MWNT/PPy-*p*TS 5CV platforms resulted in a significant increase in total cell nuclei (A) as well as a significant increase in myoblast fusion (B), represented by percentage multinucleation. Error bars represent SEM.

neurotrophins.[11,17] Previous studies in other laboratories have also demonstrated that electrical stimulation can prime myoblasts for contractile activity through increased expression of genes associated with myogenic differentiation.[26–28,36,37] From this aspect, the use of conductive surfaces provides an additional level of cellular manipulation in vivo or ex vivo. However, to the best of our knowledge, the use of electrically conductive nanostructured platforms to deliver electrical stimulation for primary muscle regeneration has not been previously reported.

The ability to control the development of myoblasts into orientated myotubes is crucial for effective muscle engineering. In vitro culture of myoblasts results in the formation of randomly distributed myotubes which does not reflect native muscle architecture, however micro and nanopatterned surfaces can be used to enhance myotube alignment.[8,38] Here we combined the ability to influence cellular orientation through controlled nanostructure with the ability to influence cellular behaviour through electrical stimulation. It was anticipated that the influence of nanostructure on surface properties may influence myoblast growth behaviour, particularly due to the requirement of differentiating myoblasts to fuse with other myoblasts in close proximity to form myotubes. However, no significant differences in myotube length, size and multinucleation was found between nanostructured surfaces and non-nanostructured surfaces, suggesting that the nanostructured PPy-*p*TS used in this study does not have an inhibitory effect on myotube formation. It was also envisaged that MWNT arrays deposited with 5 to 25 CV cycles of PPy-*p*TS would have progressively diminishing nanostructure that would influence the extent of myotube alignment. This was indeed the case with significantly less myotube orientation seen on MWNT surfaces with increased deposition of PPy-*p*TS. Thicker PPy films are known to possess different physical properties to their thinner counterparts, including differences in wettability and surface roughness and this can have a significant effect on cellular response.[30] This has been elegantly demonstrated by the Schmidt group where significant differences in cell viability and behaviour (e.g., cell spreading) are seen on PPy films of varying thickness, depending on the dopant used.[39] Our previous studies of PPy-*p*TS have also shown that very thick films (1850 nm) are significantly rougher than thinner films (16.2 nm), however large differences in wettability were not observed on these polymers despite observed differences in cellular response.[30] Therefore, in the current study it is feasible that the observed reduction in myoblast alignment on progressively thicker PPy-*p*TS coatings could be due to a progressive dissipation of nanotopography and consequent "randomisation" of topographical cues in samples with thicker coatings (35 CV cycles) of PPy-*p*TS. However, further studies of the nature of PPy-*p*TS growth on MWNT aerogel sheets are required to fully characterise this phenomenon.

The correlation of progressive dissipation of nanotopography with decreased myotube orientation highlights the importance of nano-topographical cues to the promotion of linear myogenic growth. Whilst myotube alignment was most evident on the bare MWNTs, this was accompanied by much lower levels of differentiation, smaller myotube footprint and length indicating that the beneficial effects of the nanotopography may be offset by the inherent properties of the MWNTs, such as hydrophobicity. In addition, a reduced number of myoblasts were observed to adhere to MWNT surfaces, however this did not reach a statistically significant level. Nevertheless, reduced cell attachment may have had an influence on the significantly reduced levels of differentiation observed on MWNT surfaces. These observations highlight the superior cytocompatibility of PPy-*p*TS compared to MWNT. This was evident in films with minimal (5 CV cycles) of PPy-*p*TS deposited on the MWNT, which improved surface affinity and thereby, the differentiation of primary muscle cells.

A smaller myotube footprint represents a reduced ability of the myotubes to spread over the surface of the MWNT substrates. This may be influenced by the ability of myotubes to create focal adhesions with the MWNT surface. Reduced cell spreading and lack of focal adhesions has been observed on surfaces suboptimal for cellular adhesion. This has been recently demonstrated to occur in stem cells[40] and similar mechanisms have been described in myoblasts.[41] There are numerous proteins involved in the formation of focal adhesions including integrins, talins and focal adhesion kinases, all of which play a role in cell adhesion and spreading.[42,43] Whilst the precise molecular mechanisms by which myoblasts adhere to conductive platforms described in this study are yet to be characterised, it is likely to involve such molecules and it would be of interest

to analyse the expression and distribution of these complexes on electrically active and nanostructured materials in future studies.

Previous studies on nanostructured platforms using C2C12 cells have demonstrated a significant increase in myotube length on aligned nanostructured templates,[8] which somewhat differs from the findings presented here. In our study we compare myotube length on substrates that vary from nanostructured and orientated surfaces to smooth platforms and as such did not compare the effects of non-orientated nanostructure on primary myoblasts. It is feasible that random topography could have some inhibitory effect on myotube formation due to nanostructural features orientated across the line of myotube growth, which could account for the differences reported by Huang[8] and those reported here. In addition, our study investigated the behaviour of primary myoblasts rather than myoblast cell lines whose transformed state introduces potential differences in behavioural response compared to primary myoblasts. This latter difference is important when evaluating replicative growth and differentiation whereby transformed cells are known to have lost some of their capability to respond to external stimuli (particularly in their response to the substratum) in a biologically relevant manner.[44] This issue is highlighted by Langelaan and colleagues who showed striking differences in the maturation levels of C2C12s and primary myoblasts in response to electrical stimulation, with primary cells undergoing more advanced maturation, suggesting a greater sensitivity to electrical stimulus.[45] This emphasises the potential for missing relevant biological context in cellular response to external stimuli such as electrical stimulation using cell lines rather than primary cells.

Application of electrical stimulation to myoblasts on nanostructured MWNT/PPy-*p*TS platforms led to significant enhancements in total myo-nuclear density and myoblast differentiation. These results indicate that on these platforms, electrical stimulation served to increase the proliferative activity of primary myoblasts and enhanced the formation of myotubes via myoblast fusion. Whilst it remains unclear as to whether these increases in myoblast fusion are primarily due to increased cell density (arising from increased proliferative activity) or whether there is a synergistic effect of electrical stimulation on cell proliferation and myoblast fusion, it is nevertheless apparent from our results that electrical stimulation on these platforms promotes an enhanced myoregenerative response. Further studies will define the precise mechanisms giving rise to these effects on myogenic cell growth and the potential for this paradigm to be applied in vivo.

The nanostructured conductive platforms presented in this study utilised aligned MWNT sheets as templates for providing nanostructured topography. Taking advantage of the ability to control nanostructure and the inherent biocompatibility of PPy-*p*TS, we demonstrate in the first instance, that this platform can be used to control the orientation of myotube differentiation. In addition, this platform can be used to deliver trophic electrical stimulation directly to primary myoblasts to influence their rate of differentiation and cell division. These findings are important in the myoregenerative field, and also in fields where electrical activity and orientation is known to influence cellular behaviour, such as in neural[11,12,45,46] and cardiac[49] tissues and in bionic devices that monitor or otherwise affect biological activity for therapeutic purposes, such as the bionic ear and the cardiac pacemaker.[50] The novel conductive platform described in this study provides the basis for nanostructured electrically active surfaces for controlled myo-regenerative applications in vivo or for an effective implantable bionic device interface with muscle tissue.

Experimental Section

Platform Synthesis and Characterization: MWNT aerogel sheets, having a density of ≈0.0015 g cm^{-3}, were drawn from MWNT forests (tightly packed vertically grown arrays of MWNT), deposited onto Au mylar substrate then densified to ≈0.5 g cm^{-3} using surface tension effects associated with infiltration and evaporation of ethanol, as previously described.[23] Where required, the surfaces of individual MWNT bundles in the sheet and the exposed surface of the underlying Au mylar substrate were coated with PPy-*p*TS by electrochemical polymerization of a solution containing pyrrole monomer (0.05 M) and *p*TS (0.0125 M) by CV. Unless otherwise stated, 5 CV cycles at the potential range of –300 to 850 mV and 50 mV s^{-1} scan rate were used for deposition of PPy-*p*TS. To evaluate the effect of orientated nanotopography on muscle cell alignment, the PPy-*p*TS coat thickness was controlled by varying the number of cycles during CV deposition. MWNT arrays were subjected to 5, 10, 25 or 35 CV cycles of PPy-*p*TS deposition. It was important to ensure complete coverage of the Au mylar and MWNTs to differentiate the effects between the gold, MWNTs and the MWNT/PPy-*p*TS surfaces during cell culture. It was found that 5 CV cycles of PPy-*p*TS deposition was the minimum amount of deposition to ensure this coverage, while minimizing disruption of the nanostructure in the sheets. Atomic force microscopy (AFM) and scanning electron microscopy (SEM) analysis indicated that increasing the number of CV cycles increased the thickness of PPy-*p*TS on the MWNTs and on the Au mylar substrate. The electrochemical behaviour of conductive substrates was analysed by CV under biological conditions (i.e., in myoblast proliferation media).

Cell Culture and Electrical Stimulation: A 4 well polystyrene chamber was attached to the scaffold surface to facilitate cell culture. The scaffold was designed to allow electrical stimulation via two separate strips, as previously described.[11] For analysis of primary myoblast response to the scaffolds, myoblasts were prepared from B10.129S4Gt(ROSA)26 male mice at 5–6 weeks of age (Bioresources Center, St. Vincent's Hospital Melbourne, Australia) and seeded onto platforms at 30 000 cells/cm^2 in myoblast proliferation medium, as previously described.[18] The cells were cultured for 24 hours to allow complete adhesion onto prepared surfaces. Myoblasts were then cultured under differentiation conditions for the required length of time prior to immunostaining, as previously described.[18]

For electrical stimulation experiments, myoblasts were seeded in two groups each at 30 000 cells/cm^2 cell density onto similarly prepared MWNT/5CV PPy-*p*TS platforms as described above, and allowed to adhere and proliferate for 48 hours before the media was changed to induce differentiation. Myoblasts were allowed to adjust to differentiation conditions for 24 hours prior to electrical stimulation. An auxillary reference electrode and a cathode were attached to the Au mylar strips used as templates for MWNT fiber and PPy-*p*TS deposition. The differentiating myoblasts were then stimulated with 0.125 mA cm^{-2} bipolar square wave 2 ms pulses separated by a 2 µs interruption in applied current, at a frequency of 10 Hz using an Accupulser interfaced with an e-corder system (World Precision Instruments). Electrical stimulation was applied for 8 hours per 24 hours period for 3 days under 5% CO_2 at 37 °C, before cells were fixed for immunostaining and analysis. The stimulation parameters chosen for this study were adapted from Langelaan[45] and Zhang[46] and from our previous experiments with stimulation of neural cells on similar platforms.[11,12]

DOI: 10.1002/adhm.201200102

Immunostaining and Analysis: The cells were fixed and immunostained for desmin, an intermediate filament protein specific to muscle, as previously described.[47] All specimens were visualized using an Olympus IX-70 fluorescent microscope and images taken using Spot Advanced 4.0.9 software (Diagnostic Instruments). Random non-overlapping fields of fluorescently labelled myotubes were taken at 100× magnification. Only myotubes that were clearly distinguishable from others were included in the analysis and for each parameter a minimum number of 40 myotubes were analysed. Myotube length and surface area was assessed using the "Add Measurement" function in Spot Advanced software (Diagnostic Instruments). Myotube alignment was assessed by measuring the angle of the myotubes relative to the axis of the MWNTs. A minimum myotube alignment value of 0° denoted parallel alignment with the MWNTs array and a maximum of 90° represented perpendicular alignment. An arbitrary axis of alignment was used for analysis of the platform in the absence of the MWNTs. Myotube differentiation was assessed by calculating the percentage of nuclei within myotubes (fusion of two or more myoblasts) as a percentage of total nuclei (from both myoblasts and myotubes) per field. Cell numbers were quantified using the cell count function in ImageJ (NIH).[48] At least 10 fields were counted per sample and the results from two independent experiments were combined for statistical analysis.

All data analysis was carried out using GraphPad prism V5.04. Data sets obtained from myotube length, surface area and myotube:MWNTs axis angle, were first assessed for normality using D'Agostino and Pearson omnibus normality test. Analysis for significance was then performed using ANOVA (two-tailed) or by student *t*-test. Representation of significance is denoted: $* p < 0.05$, $** p < 0.01$, $*** p < 0.001$.

Supporting Information

Supporting Information is available from the Wiley Online Library or from the author.

Acknowledgements

The authors thank the ACES Bionics Group for helpful discussions, the Australian Research Council (ARC) and National Health and Medical Research Council (NHMRC) of Australia for financial support and the ANFF Materials Node for their provision of research facilities. This work was also supported by ARC APD Fellowship DP098753 (J.M.R.), ARC Federation Fellowship (G.G.W.). J.M.R acknowledges the ARC Nanotechnology Network for the Overseas Travel Fellowship Award. R.H.B and R.O.-R. acknowledge support from Air Force Office of Scientific Grant FA9550-09-1-0537 and Robert A. Welch Foundation grant AT-0029.

Received: March 31, 2012
Revised: July 2, 2012
Published online:

[1] Y. Chen, S. Zhou, Q. Li, *Biomaterials* **2011**, *32*, 5003.
[2] T. Fuhrmann, L. M. Hillen, K. Montzka, M. Woltje, G. A. Brook, *Biomaterials* **2010**, *31*, 7705.
[3] T. Dvir, B. P. Timko, D. S. Kohane, R. Langer, *Nat. Nanotechnol.* **2011**, *6*, 13.
[4] M. J. Webber, J. A. Kessler, S. I. Stupp, *J. Intern. Med.* **2010**, *267*, 71.
[5] J. Ma, X. He, E. Jabbari, *Ann. Biomed. Eng.* **2011**, *39*, 14.
[6] Y. I. Cho, J. S. Choi, S. Y. Jeong, H. S. Yoo, *Acta Biomater.* **2010**, *6*, 4725.
[7] N. F. Huang, R. J. Lee, S. Li, *Am. J. Transl. Res.* **2010**, *2*, 43.
[8] N. F. Huang, S. Patel, R. G. Thakar, J. Wu, B. S. Hsiao, B. Chu, R. J. Lee, S. Li, *Nano. Lett.* **2006**, *6*, 537.
[9] A. Ferrari, M. Cecchini, A. Dhawan, S. Micera, I. Tonazzini, R. Stabile, D. Pisignano, F. Beltram, *Nano. Lett.* **2011**, *11*, 505.
[10] N. W. Kam, E. Jan, N. A. Kotov, *Nano. Lett.* **2009**, *9*, 273.
[11] A. F. Quigley, J. M.Razal, B. C. Thompson, S. E. Moulton, M. Kita, E. L. Kennedy, G. M. Clark, G. G. Wallace, R. M. I Kapsa, *Adv. Mater.* **2009**, *21*, 4393.
[12] X. Liu, J. Chen, K. J. Gilmore, M. J. Higgins, Y. Liu, G. G. Wallace, *J. Biomed. Mater. Res. A* **2010**, *94*, 1004.
[13] M. Bhattacharya, P. Wutticharoenmongkol-Thitiwongsawet, D. T. Hamamoto, D. Lee, T. Cui, H. S. Prasad, M. Ahmad, *J. Biomed. Mater. Res. A* **2011**, *96*, 75.
[14] C. A. Abdullah, P. Asanithi, E. W. Brunner, I. Jurewicz, C. Bo, C. L. Azad, R. Ovalle-Robles, S. Fang, M. D. Lima, X. Lepro, S. Collins, R. H. Baughman, R. P. Sear, A. B. Dalton, *Nanotechnology* **2011**, *22*, 205102.
[15] G. G. Wallace, S. E. Moulton, G. M. Clark, *Science* **2009**, *324*, 185.
[16] B. C. Thompson, S. E. Moulton, J. Ding, R. Richardson, A. Cameron, S. O'Leary, G. G. Wallace, G. M. Clark, *J. Controlled Release* **2006**, *116*, 285.
[17] B. C. Thompson, R. T. Richardson, S. E. Moulton, A. J. Evans, S. O'Leary, G. M. Clark, G. G. Wallace, *J. Controlled Release* **2010**, *141*, 161.
[18] J. M. Razal, M. Kita, A. F. Quigley, E. Kennedy, S. E. Moulton, R. M. I. Kapsa, G. M. Clark, G. G. Wallace, *Adv. Funct. Mater.* **2009**, 3381.
[19] S. Meng, Z. Zhang, M. Rouabhia, *J. Bone Miner. Metab.* **2011**.
[20] E. M. Stewart, X. Liu, G. M. Clark, R. M. Kapsa, G. G. Wallace, *Acta Biomater.* **2011**.
[21] T. R. Nayak, L. Jian, L. C. Phua, H. K. Ho, Y. Ren, G. Pastorin, *ACS Nano* **2010**, *4*, 7717.
[22] K. Matsumoto, C. Sato, Y. Naka, R. Whitby, N. Shimizu, *Nanotechnology* **2010**, *21*, 115101.
[23] M. Zhang, S. Fang, A. A. Zakhidov, S. B. Lee, A. E. Aliev, C. D. Williams, K. R. Atkinson, R. H. Baughman, *Science* **2005**, *309*, 1215.
[24] P. Galvan-Garcia, E. W. Keefer, F. Yang, M. Zhang, S. Fang, A. A. Zakhidov, R. H. Baughman, M. I. Romero, *J. Biomater. Sci., Polym. Ed* **2007**, *18*, 1245.
[25] A. R. Gillies, R. L. Lieber, *Muscle Nerve* **2011**, *44*, 318.
[26] Y. Kawahara, K. Yamaoka, M. Iwata, M. Fujimura, T. Kajiume, T. Magaki, M. Takeda, T. Ide, K. Kataoka, M. Asashima, L. Yuge, *Pathobiology* **2006**, *73*, 288.
[27] J. R. Crew, K. Falzari, J. X. DiMario, *Exp. Cell Res.* **2010**, *316*, 1039.
[28] M. Flaibani, L. Boldrin, E. Cimetta, M. Piccoli, C. P. De, N. Elvassore, *Tissue Eng. Part A* **2009**, *15*, 2447.
[29] H. Zhao, W. E. Price, G. G. Wallace, *J. Membr. Sci.* **1998**, *148*, 161.
[30] K. J. Gilmore, M. Kita, Y. Han, A. Gelmi, M. J. Higgins, S. E. Moulton, G. M. Clark, R. Kapsa, G. G. Wallace, *Biomaterials* **2009**, *30*, 5292.
[31] X. Wang, X. Gu, C. Yuan, S. Chen, P. Zhang, T. Zhang, J. Yao, F. Chen, G. Chen, *J. Biomed. Mater. Res. A* **2004**, *68*, 411.
[32] L. Cen, K. G. Neoh, E. T. Kang, *Biosens. Bioelectron.* **2003**, *18*, 363.
[33] T. Ahuja, I. A. Mir, D. Kumar, Rajesh, *Biomaterials* **2007**, *28*, 791.
[34] B. C. Thompson, J. Chen, S. E. Moulton, G. G. Wallace, *Nanoscale* **2010**, *2*, 499.
[35] B. C. Thompson, S. E. Moulton, R. T. Richardson, G. G. Wallace, *Biomaterials* **2011**, *32*, 3822.
[36] I. Jun, S. Jeong, H. Shin, *Biomaterials* **2009**, *30*, 2038.
[37] V. Aas, S. Torbla, M. H. Andersen, J. Jensen, A. C. Rustan, *Ann. N.Y. Acad. Sci.* **2002**, *967*, 506.
[38] E. Rebollar, I. Frischauf, M. Olbrich, T. Peterbauer, S. Hering, J. Preiner, P. Hinterdorfer, C. Romanin, J. Heitz, *Biomaterials* **2008**, *29*, 1796.
[39] J. M. Fonner, L. Forciniti, H. Nguyen, J. D. Byrne, Y. F. Kou, J. Syeda-Nawaz, C. E. Schmidt, *Biomed. Mater.* **2008**, *3*, 034124.
[40] B. Trappmann, J. E. Gautrot, J. T. Connelly, D. G. Strange, Y. Li, M. L. Oyen, M. A. Cohen Stuart, H. Boehm, B. Li, V. Vogel, J. P. Spatz, F. W. Watt, W. T. Huck, *Nat. Mater.* **2012**, *11*, 642.

[41] O. Thompson, C. J. Moore, S. A. Hussain, I. Kleino, M. Peckham, E. Hohenester, K. R. Ayscough, K. Saksela, S. J. Winder, *J. Cell Sci.* **2010**, *123*, 118.
[42] M. A. Partridge, E. E. Marcantonio, *Mol. Biol. Cell* **2006**, *17*, **4237**.
[43] L. Kornberg, H. S. Earp, J. T. Parsons, M. Schaller, R. L. Juliano, *J. Biol. Chem.* **1992**, *267*, 23439.
[44] H. B. Wang, M. Dembo, Y. L. Wang, *Am. J. Physiol. Cell Physiol.* **2000**, *279*, C1345.
[45] M. L. Langelaan, K. J. Boonen, K. Y. Rosaria-Chak, D. W. van der Schaft, M. J. Post, F. P. Baaijens, *J. Tissue Eng. Regener. Med.* **2011**, *5*, 529.
[46] B. T. Zhang, S. S. Yeung, Y. Liu, H. H. Wang, Y. M. Wan, S. K. Ling, H. Y. Zhang, Y. H. Li, E. W. Yeung, *BMC Cell Biol.* **2010**, *11*, 87.
[47] M. L. Costa, R. Escaleira, A. Cataldo, F. Oliveira, C. S. Mermelstein, Brazilian *J. Med. Biol. Res.* **2004**, *37*, 1819.
[48] M. D. Abramoff, P. J. Magalhaes, S. J. Ram, *Biophotonics Int.* **2004**, *11*, 36.
[49] H. T. Au, I. Cheng, M. F. Chowdhury, M. Radisic, *Biomaterials* **2007**, *28*, 4277.
[50] G. G. Wallace, S. Moulton, M. Higgins, R. M. I. Kapsa, *Organic Bionics*, Wiley-VCH, Weinheim, Germany **2012**.

Adv. Healthcare Mater. **2012**,
DOI: 10.1002/adhm.201200102